

## GROUND STATE ENERGY OF HYDRO HELIUM CATION (2+) ( $He^{++}H$ ) CALCULATED BY QUANTUM MONTE CARLO METHOD

Muhammad Rameez<sup>\*1</sup>, Muhammad Mujtaba Zafar<sup>2</sup>, Sidra Khan<sup>3</sup>, Faisal Aziz<sup>4</sup>

<sup>\*1</sup>Department of Physics, University of Karachi

<sup>2</sup>Department of Physics, Ned University of Engineering and Technology

<sup>3</sup>Department of Physics, Federal Urdu University of Science and Technology

<sup>4</sup>Department of Physics, Ned University of Engineering and Technology

<sup>1</sup>rameez-mateen@hotmail.com, <sup>2</sup>mujtaba.zafar93@hotmail.com, <sup>3</sup>Sidrakhan18@hotmail.com,  
<sup>4</sup>faisal91aziz@gmail.com

DOI: <http://doi.org/10.5281/zenodo.19690417>

### Keywords

Hartree-Fock Method, DMC (Diffusion Monte Carlo), Ground state energy, Slater-Jastrow wave function and Quantum Monte Carlo (QMC).

### Article History

Received: 23 February 2026

Accepted: 04 April 2026

Published: 21 April 2026

Copyright @Author

Corresponding Author: \*

Muhammad Rameez

### Abstract

In the below study, a well-known theoretically model Quantum Monte Carlo (QMC) is used to determine ground state energy of hydro helium cation (2+) ( $He^{++}H$ ). We have used (DMC) method Diffusion Quantum Monte Carlo, to find out energy of hydro helium cation (2+) ( $He^{++}H$ ) for ground state. The Slater-Jastrow trial wave function serves as the basis for our calculation. we used importance sampling technique, to improve the accuracy and using metropolis algorithm for Implementation of method. A Python program is developed for hydro helium cation (2+) ( $He^{++}H$ ). The energy obtained by using DMC methods is -3.45833 Hartree. Comparison is also made by DHF (Dirac Hartree-Fock) and ROHF (Restricted Open Shell Hartree Fock) methods; this article is helpful for understanding ground state energy and the QMC (Quantum Monte Carlo) method.

### INTRODUCTION

The application and properties of ground states of many electron systems have great implications in many fields of research. The spectroscopic data signify research areas in both theoretical and experimental fields like fine structure, transition probabilities, Rydberg levels, ionization potentials, etc. We must use approximation to solve the Schrodinger Equation for a system with multiple electrons. The approximation was developed by J. Robert and Max Born, and where the wave functions of electrons and nuclei are separated without considering the interaction between electrons and nuclei. This can be

accomplished by using the Time-Independent Schrödinger equation. They computed the hydrogen molecule's binding energy and internuclear separation [1]. Hartree-Fock method is also important tool. [2]. other approximations are (Variational Quantum Monte Carlo) QMC method, in these integrals and Variational parameters are used with Monte Carlo integration and Metropolis Algorithms to calculate energies. [3]. One calculated the energy (ground state) of hydro helium cation (2+) ( $He^{++}H$ ) utilizing the Simulation of DMC, Diffusion Quantum Monte Carlo. We obtain data through simulations and then, we analyze the reliability of our methods in approximating

and simulating by comparing our values against the results obtained experimentally. On the case where we used QMC, our results are based on trial wave function. [4] The lattice energy ( $E_{latt}$ ) of different molecular crystals was successfully determined by Andrea Zenet et al. in (2018) using the Diffusion Quantum Monte Carlo method and then comparing their results against experimental results. [5]. O. Withams et al. (2018) used VMC and DMC to determine the binding energy of indirect trions and biexcitons [6]. In 2018, S. B. Doma and associates used VMC in calculating the ground state energy of free and confined hydrogen molecule ( $H_2$ ) [7]. In 2018, Astrakhantsev et al. used quantum Monte Carlo simulation in evaluating the dielectric permittivity of suspended graphene over different temperatures and extrapolated the results at zero separation [8]. The authors John Trail et al. (2017) obtained the values of Helmholtz energy, which can be defined as the sum of the electronic energy and harmonic vibration energy of the system under consideration, for various forms of  $TiO_2$  by the methods of diffusion quantum Monte Carlo and density functional theory [9]. For DMC calculations, Slater-Jastrow trial wave functions were chosen [9]. The total energy of lithium dimers ( $Li_2^+$  and  $Li_2^-$ ) was obtained by Saeed Nasiri and Mansour Zahedi (2017) by applying the method of diffusion quantum Monte Carlo (DMC). The trial wave functions were defined as a product of multi-determinant wave-functions and Jastrow correlation function [10]. With the help of diffusion quantum Monte Carlo calculations, Szymszewski et al. (2017) evaluated the binding energy of trions and biexcitons in 2D semiconductors. [11]. Saeed Nasiri and Mansour Zahedi (2017) used the Diffusion Quantum Monte Carlo (DMC) technique to compute the ground-state total energies of atoms and molecules. Multi-determinant trial wave-functions were used in their computations [12]. Michel Caffarel et al. (2017) computed the ground-state energy of the water molecule via the Fixed-Node Quantum Monte Carlo technique. Rather than making use of the traditional Jastrow correlation factor, trial wave-functions were generated via chosen

Configuration Interaction computations [13]. As noted by S. B. Doma and colleagues in their study published in 2016, the ground state energies of the hydrogen molecule and its molecular ions were computed using the Variational Monte Carlo approach in situations where there is a presence and absence of magnetic fields [14]. On their part, Wirawan Purwanto and colleagues evaluated the dissociation energy of the molybdenum molecule using the Auxiliary-Field Quantum Monte Carlo procedure [15]. Andrew D. Powell et al., on the other hand, evaluated PECs of and using the Fixed-Node Diffusion Monte Carlo method in two ways. The first approach involved high precision but required significant computational resources, while the second approach was less rigorous and involved less time-consuming optimization. In both approaches, they computed energies by varying both the bond lengths and the number of determinants, as well as by keeping the number of determinants constant while changing bond lengths. Their results showed close agreement with spectroscopically accurate curves [16]. R. Nazarov and colleagues (2016) determined the dissociation energies of various molecules and solids using Pseudopotentials in combination with fixed-node Diffusion Monte Carlo [17]. Katharina Doblhoff-Dier et al. (2016) employed Diffusion Monte Carlo (DMC) to investigate the potential effects of locality and pseudopotential errors on transition metal-containing dimers (TMCDs), utilizing a single-determinant Slater-Jastrow trial wave function [18]. Sharma et al. (2016) investigated how mass asymmetry affects the ground state characteristics of an electron-hole bilayer (EHL) through the use of the Variational Monte Carlo technique [19]. N. L. Moreira et al. (2016) employed fixed-node Diffusion Quantum Monte Carlo (DMC) to determine the total energy of small lithium clusters doped with either a hydrogen or fluorine atom [20]. In 2016, Sylvester A. Ekong and David A. Oyegoke employed Variational Quantum Monte Carlo (VMC) and Diffusion QMC techniques to determine the total energy and bond lengths of polyatomic organic molecules [21]. S. B. Doma

and colleagues (2016) employed Variational Quantum Monte Carlo (VMC) method to compute the ground state energy of the helium (He) atom and He-like ions up to  $Z = 10$  in the presence of an external magnetic field with strengths ranging from  $\gamma = 0-100$  a.u. [22]. In 2015, K.M. Ariful Kabir et al. employed Variational Quantum Monte Carlo (VMC) method to determine the ground state energy of the Beryllium (Be) and Boron (B) atom [23].

### Theory

We have applied the DMC approach in order to determine the ground state energy of Hydro

Helium cation ( $2+$ ) ( $He^{++}H$ ). The trial wave function of the DMC approach is constructed using the Slater-Jastrow form along with the importance sampling method in order to enhance the accuracy in DMC approach and HF approach, the trial wave function will be formed using the basis set of Slater Type Orbitals (STOs). Sampling will be done using the Metropolis approach. The Python Programming Language has been used for the implementation of the code of both methods.

### Algorithm (Diffusion Monte Carlo)

The Diffusion Monte Carlo algorithm employed in this thesis in estimating the ground state energy of systems follows the algorithm described in [24][25].

#### 1. In the first step in simulation

in the time  $0$  to  $t$

the walkers from  $0$  to  $N_{walkers}$

#### Diffusion:

For the particles  $0$  to  $N_{particles}$

(a). The initial walkers  $N_i$  are set up in configuration space forming an initial wave function using Algorithm.

(b). The  $E_R$  (reference energy) is assumed to be the average potential of walkers.

#### 2. In each cycle of simulation

(a). the value of time  $\tau$  is determined by a small increment  $\nabla\tau$ .

(b). the new location of walkers is obtained using any random variable from a Gaussian distribution with

mean  $0$  and standard deviation  $\sigma = \sqrt{\frac{\hbar\nabla\tau}{m_n}}$

(c). The  $E_R$  is obtained by the formula,

$$E_R = \langle V \rangle + \alpha \left( 1 - \frac{N}{N_i} \right) \quad (1)$$

$\langle V \rangle$  defined as the average potential energy of the entire walker,

$N$  defines as the current number of walkers.

(d). for each walker a value  $m_n$  is determined through

$$m_n = [W(x_n) + U] \tag{2}$$

$U$  is a randomly generated value that is uniformly distributed between 0 and 1, while

$W(x_n)$  represents the weight of the walker located at point  $x_n$ ,  $n = 1,2,3, \dots$  defined by

$$W(x_n) = e^{\frac{-(V(x)-E_R)\Delta\tau}{\hbar}} \tag{3}$$

In case,  $m_n = 0$ , death of particle occurs.

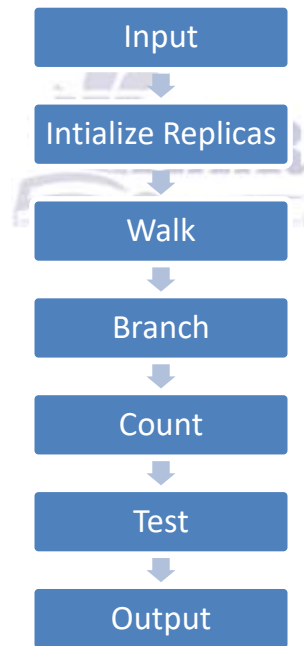
In case,  $m_n = 1$ , the next diffusion takes place, but the particle is unaffected.

In case,  $m_n > 1$ , diffusion takes place, and the Birth of Particle occurs. However, in one cycle only up to a maximum of two particles can be created in order to manage the increase.

3. Repetition of the configuration moves for the required number of steps.
4. Ground state energy is determined by averaging the reference energies of all the iterations.
5. Repetition of the procedure until enough data is collected.

**DMC Flow Diagram**

Below flow chart illustrates the flow of the Diffusion Monte Carlo (DMC) method implemented in the python program, where each block represents a specific task.



• **Input**

In the beginning, there are some input data which consist of number of particles, iterations, coordinates, value of time step  $\nabla\tau$ , number of walkers and energy reference value.

• **Intialize Replicas**

Estimations are made for diffusion and branching in NNN dimensional matrix format where constraints have been imposed for creating the new particles for not allowing unlimited branching.

- **Walk**

Diffusion process occurs for performing the function of generating new successive positions  $x_n$  for values of  $n$  by generating a sequence of random numbers  $\rho_n$ ,  $n = 1, 2, 3, \dots$ .  $x_0, x_1 = x_0 + \sigma\rho_1, x_2 = x_1 + \sigma\rho_2$ , where  $\sigma$  is the standard deviation from the mean position.

- **Branch**

The birth-death dynamics are executed through a process influenced by diffusion and the associated replication factor  $m_n$ .

- **Count**

This approach facilitates the calculation of the ground-state wave function. The calculation proceeds once a stationary regime is attained and energy convergence is observed, with energy values remaining almost unchanged over time steps.

- **Test**

Assess convergence and the attainment of a stationary state. If these conditions are not met, revert to Step 3 and continue the iteration.

- **Output**

The reported simulation results are the average energy derived from the reference energies at each successive iteration [26].

### Result and Discussion

The Outcome from the calculations performed on DMC, DHF, and ROHF using Python Language for Hydro helium cation two ( $He^{++}H$ ) is shown below in tables along with their energies. All the energies are expressed in eV (electron volt) Unit. Moreover, PECs for DMC, DHF, and ROHF have been provided below.

**Table I: Calculated Energies of ( $He^{++}H$ ) by using Diffusion Monte Carlo technique**

Bond Length ( $\times 10^{-10}m$ )	Energy (eV)
0.05	-132.298
0.1	-120.82
0.2	-110.024
0.3	-101.131
0.4	-94.106
0.5	-88.3494
0.6	-83.8628
0.7	-79.9068
0.8	-76.9391
0.9	-74.0781
1.0	-71.6563
1.1	-69.1311
1.2	-67.0176
1.3	-64.6823
1.4	-63.7188

Table II: Calculated Energies of (He<sup>++</sup>H) by using Dirac Hartree-Fork Simulation

Bond Length ( $\times 10^{-10}m$ )	Energy (eV)	Bond Length ( $\times 10^{-10}m$ )	Energy (eV)	Bond Length ( $\times 10^{-10}m$ )	Energy (eV)
0.1	315.6005144	0.3	-65.72896962	0.6	-79.03727215
0.1	242.0180466	0.4	-66.95079931	0.6	-79.12029821
0.1	187.9128741	0.4	-68.06754645	0.7	-79.19401771
0.1	146.5733938	0.4	-69.08898078	0.7	-79.25911527
0.1	114.0526766	0.4	-70.0238091	0.7	-79.31622601
0.1	87.87831043	0.4	-70.87981335	0.7	-79.36594123
0.1	66.42270712	0.4	-71.66396835	0.7	-79.40880926
0.1	48.5705457	0.4	-72.3825406	0.7	-79.44534138
0.1	33.53176521	0.4	-73.04117458	0.7	-79.47601407
0.1	20.73087012	0.4	-73.64496507	0.7	-79.5012706
0.2	9.738544814	0.4	-74.19851978	0.7	-79.52152486
0.2	0.227848127	0.5	-74.70601429	0.7	-79.53716271
0.2	-8.05472433	0.5	-75.17123889	0.8	-79.5485447
0.2	-15.3088746	0.5	-75.59763881	0.8	-79.55600715
0.2	-21.6941368	0.5	-75.98835016	0.8	-79.55986328
0.2	-27.3395417	0.5	-76.34623095	0.8	-79.56040669
0.2	-32.3505967	0.5	-76.67388886	0.8	-79.55791031
0.2	-36.8144122	0.5	-76.97370597	0.8	-79.55262967
0.2	-40.8035278	0.5	-77.24785974	0.8	-79.54480231
0.2	-44.3788102	0.5	-77.49834231	0.8	-79.53465055
0.3	-47.5916774	0.5	-77.72697793	0.8	-79.52238148
0.3	-50.4858304	0.6	-77.93543957	0.8	-79.5081891
0.3	-53.0986152	0.6	-78.12526058	0.9	-79.49224812
0.3	-55.4621079	0.6	-78.29785025	0.9	-79.47473132
0.3	-57.6039846	0.6	-78.45450301	0.9	-79.45579192
0.3	-59.5482305	0.6	-78.59640965	0.9	-79.43557548
0.3	-61.315714	0.6	-78.72466704	0.9	-79.41421616
0.3	-62.9246642	0.6	-78.84028638	0.9	-79.39183941
0.3	-64.3910624	0.6	-78.94420073	0.9	-79.36856115
0.9	-79.3444897	1.1	-78.86106772	1.3	-78.43599218
0.9	-79.3197251	1.1	-78.83462396	1.3	-78.41602201
0.9	-79.29436	1.1	-78.80843951	1.3	-78.39646164
1.0	-79.2684812	1.1	-78.78253453	1.3	-78.3773108
1.0	-79.2421677	1.1	-78.75692588	1.3	-78.35856922
1.0	-79.2154946	1.2	-78.7316299	1.3	-78.34023581
1.0	-79.1885294	1.2	-78.70666071	1.3	-78.32230867
1.0	-79.1613357	1.2	-78.68203113	1.4	-78.30478643
1.0	-79.1339725	1.2	-78.65775258	1.4	-78.28766611
1.0	-79.1064936	1.2	-78.63383539	1.4	-78.27094525
1.0	-79.0789491	1.2	-78.61028855	1.4	-78.25462031
1.0	-79.0513851	1.2	-78.58711995	1.4	-78.23868831
1.0	-79.0238439	1.2	-78.56433639	1.4	-78.22314489
1.1	-78.9963653	1.2	-78.54194412	1.4	-78.20798623

1.1	-78.9689846	1.2	-78.51994752	1.4	-78.19320772
1.1	-78.9417354	1.3	-78.49835119	1.4	-78.17880473
1.1	-78.9146481	1.3	-78.47715813	1.4	-78.16477235
1.1	-78.8877504	1.3	-78.45637107		

Table III: Calculated Energies of (He<sup>++</sup>H) by using Restricted Open Shell Hartree-Fork

Bond length ( $\times 10^{-10}m$ )	Energy (eV)	Bond length ( $\times 10^{-10}m$ )	Energy (eV)	Bond length ( $\times 10^{-10}m$ )	Energy (eV)
0.1	315.6133666	0.3	-65.72461389	0.6	-79.0339276
0.1	242.0287722	0.4	-66.94651242	0.6	-79.11696373
0.1	187.9229872	0.4	-68.06332488	0.7	-79.19069193
0.1	146.582948	0.4	-69.08482097	0.7	-79.25579711
0.1	114.0617261	0.4	-70.0197078	0.7	-79.31291492
0.1	87.88690651	0.4	-70.87576756	0.7	-79.36263587
0.1	66.43089694	0.4	-71.65997535	0.7	-79.40550906
0.1	48.57837115	0.4	-72.37859794	0.7	-79.44204581
0.1	33.53926277	0.4	-73.03727927	0.7	-79.47272203
0.1	20.73807189	0.4	-73.64111466	0.7	-79.22586756
0.2	9.745478279	0.4	-74.19471209	0.7	-79.51823827
0.2	0.234537778	0.5	-74.70224715	0.7	-79.53387829
0.2	-8.048257818	0.5	-75.16751011	0.8	-79.54544477
0.2	-15.30261297	0.5	-75.59394649	0.8	-79.55272491
0.2	-21.68806404	0.5	-75.98469186	0.8	-79.55658158
0.2	-27.33364368	0.5	-76.34260503	0.8	-79.55712527
0.2	-32.34486081	0.5	-76.67029369	0.8	-79.55462889
0.2	-36.80882704	0.5	-76.97013964	0.8	-79.5493477
0.2	-40.79808386	0.5	-77.24432035	0.8	-79.5415198
0.2	-44.373498	0.5	-77.49482795	0.8	-79.53136723
0.3	-47.58648869	0.5	-77.72348725	0.8	-79.51909679
0.3	-50.48075768	0.6	-77.93197093	0.8	-79.50490142
0.3	-53.09365155	0.6	-78.12181235	0.9	-79.48896098
0.3	-55.45724681	0.6	-78.29442107	0.9	-79.47144228
0.3	-57.59922046	0.6	-78.45109125	0.9	-79.45250151
0.3	-59.54355717	0.6	-78.59301394	0.9	-79.43228344
0.3	-61.31112699	0.6	-78.72128603	0.9	-79.41092222
0.3	-62.92015857	0.6	-78.83691869	0.9	-79.38854357
0.3	-64.38663371	0.6	-78.94084529	0.9	-79.3652634
0.9	-79.34119002	1.1	-78.85773514	1.3	-78.43264028
0.9	-79.31642329	1.1	-78.83128974	1.3	-78.41266957
0.9	-79.29105628	1.1	-78.80510421	1.3	-78.39310865
1.0	-79.26517552	1.1	-78.7791976	1.3	-78.37395727
1.0	-79.23886019	1.1	-78.75358759	1.3	-78.35521514
1.0	-79.21218485	1.2	-78.7307028	1.3	-78.33688092
1.0	-79.18521781	1.2	-78.70331997	1.3	-78.3189535
1.0	-79.15802219	1.2	-78.67868903	1.4	-78.30143072
1.0	-79.13065705	1.2	-78.65440938	1.4	-78.28430985

1.0	-79.10317626	1.2	-78.63049138	1.4	-78.26758845
1.0	-79.07562988	1.2	-78.60694345	1.4	-78.25126324
1.0	-79.04806392	1.2	-78.58377376	1.4	-78.23533069
1.0	-79.02052108	1.2	-78.56098938	1.4	-78.219787
1.1	-78.99304056	1.2	-78.53859603	1.4	-78.20462807
1.1	-78.96565828	1.2	-78.51659861	1.4	-78.18984929
1.1	-78.93840742	1.3	-78.49500147	1.4	-78.17544602
1.1	-78.91131847	1.3	-78.47380787	1.4	-78.1614131
1.1	-78.88441919	1.3	-78.45301999		

**Energy Curves**

The graph showing PEC of the ground state of He<sup>++</sup>H through DMC is shown in Figure 2 below. The potential energy rises as the bond length rises up until the equilibrium bond length (or stable bond length). When the bond length is equal to the equilibrium bond length, then inter atomic forces become zero. The equilibrium bond length for He<sup>++</sup>H is  $0.4 \times 10^{-10}m$ , and its

potential energy is  $-94.11845 eV$  ( $-3.45833 Hartree$ ). At the equilibrium bond length, the repulsion force between the two protons in Helium and Hydrogen atoms balances the attraction force between the proton in Helium and electron in Hydrogen atoms. Both atoms attract each other beyond the equilibrium bond length because the repulsive force becomes attractive force.

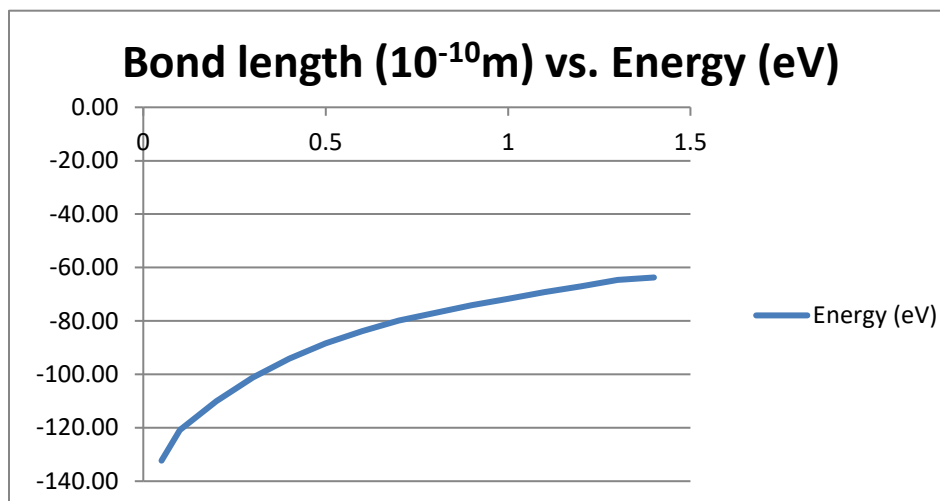


Fig 1: Using Diffusion Monte Carlo Simulation for PEC for He<sup>++</sup>H

Using HF simulations, the ground state potential energy curve (PEC) of He<sup>++</sup>H is shown in fig 1. In this case, achieving the equilibrium bond and bond length involves minimizing potential energy. Lowering the potential energy causes an increase in the electron density in the inter-atomic space, which explains the formation of a bond. The graphs are divided into three sections: before, at, and after equilibrium bond length ( $0.4 \times 10^{-10}m$ ). These graphs can be explained

by the net inter-atomic force, which is the rate of change of potential (the graph's slope).

$$\frac{dU}{dR} = -F \quad (4)$$

In case of repulsive force from equation (4), we get the negative slope and positive inter-atomic force before equilibrium bond length, since  $U$  is the potential energy,  $r$  is the bond length, and

$F$  is the inter-atomic force. The repulsion force between the protons of helium and hydrogen atoms is greater than the attractive force between the protons of helium and hydrogen atoms' electrons.

Zero slopes and inter-atomic forces are observed at equilibrium bond length. The repulsion force of hydrogen and helium atoms is equal to the attraction force. Energy associated with DHF and ROHF is  $-74.20833 \text{ eV}$  ( $-2.72674393 \text{ Hartree}$ ), and  $-74.20452 \text{ eV}$  ( $-2.7266040 \text{ Hartree}$ ), respectively.

Equation (4) indicates an attractive force, and after the equilibrium bond length, there is a very low positive slope (ideally there must be a positive slope). Repulsion between the atoms turns into attraction, and as a result, both hydrogen and helium atoms tend to move towards each other. The force of attraction decreases with increase in bond length until it reaches the bond length ( $1.4 \times 10^{-10}$ ), for dissociation. PECs using DHF and ROHF simulation are shown in Figures 3 & 4, respectively.

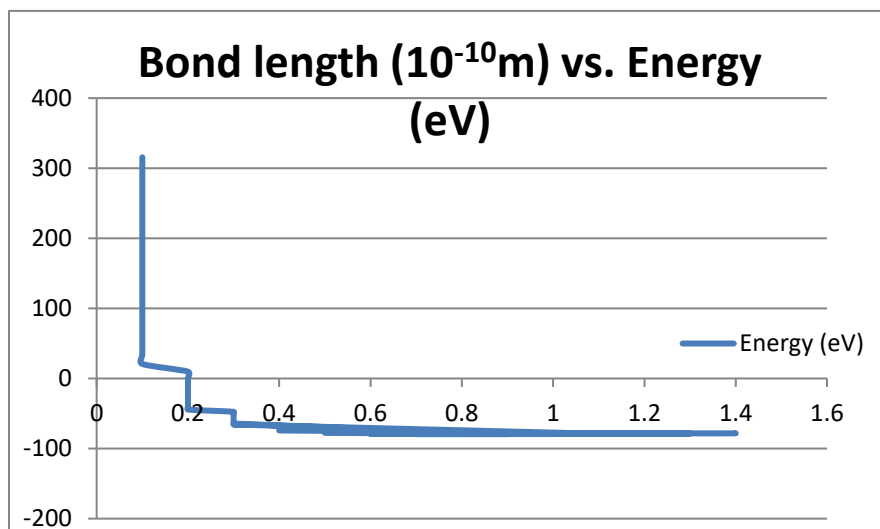


Fig 2: Using Dirac Hartree Fork Simulation for PEC for He<sup>++</sup>H

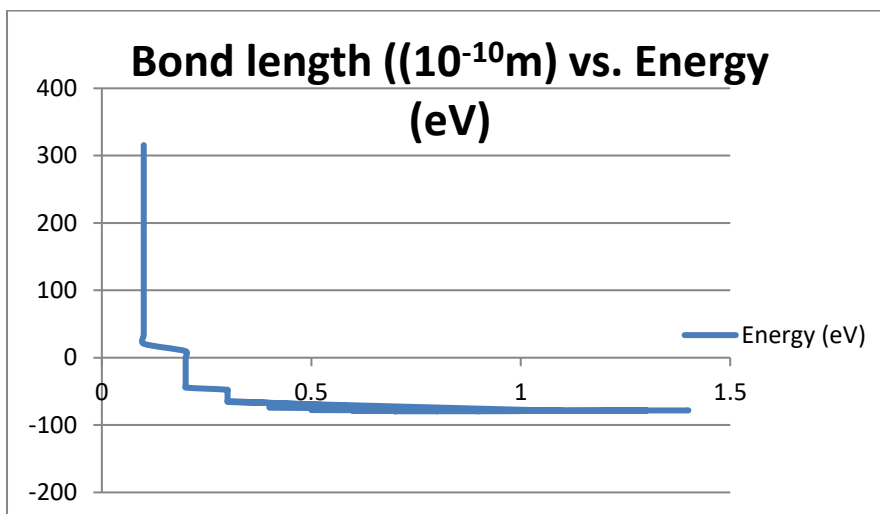


Fig 3: Using Restricted Open Shell Hartree Fork Simulation for PEC for He<sup>++</sup>H

**Conclusion**

Ground state energy calculation of hydro helium cation ( $2+$ )  $\text{He}^{++}\text{H}$  by employing diffusion quantum Monte Carlo (DMC) or approximation method that is among several types of the quantum Monte Carlo (QMC). In addition, ground state energy calculations of the hydro helium cation ( $2+$ ) were also done using the ROHF and DHF in order to make comparisons. Codes of simulation were programmed using Python programming language to do the QMC and HF processes. Accuracy of ground state energy of DMC was enhanced through development of trail wave function (Slater-Jastrow type) using importance sampling method. Trail wave function of HF was developed using STOs. Lastly, PEC curves were plotted for all three techniques: DMC, DHF and ROHF.

Energy value for the ground state of hydro helium cation ( $2+$ ) by Diffusion Monte Carlo (DMC) is  $-94.11845$  eV ( $-3.45833$  Hartree) at an equilibrium distance of  $0.4 \times 10^{-10} \text{m}$ . Energy value for Dirac Hartree Fork (DHF) is  $-74.20833$  eV (or  $-2.72674393$  Hartree), whereas for Restricted Open Shell Hartree Fork (ROHF) is  $-74.20452$  eV (or  $-2.7266040$  Hartree). Sources of error in the results obtained include: the application of the trial wave functions (Slater-Jastrow type for DMC, STOs for HF), approximation methods used in DMC and HF, limitations due to selected programming language, code used, and computing power.

**REFERENCE**

W. M. C. Foulkes, L. Mitas, R. J. Needs, and G. Rajagopal, "Quantum Monte Carlo simulations of solids," *Rev. Mod. Phys.*, vol. 73, no. 1, pp. 33–83, 2001.

H. Toffoli, "Lecture 04: The Hartree-Fock method," *Princ. Density Funct. Theory*, vol. 1, no. 7, pp. 1–9, 2012.

J. B. Anderson, "Quantum Monte Carlo :Atoms ,Molecules ,Clusters ,Liquids , and Solids," vol. 13.

A. Zen, J. G. Brandenburg, J. Klimeš, A. Tkatchenko, D. Alfè, and A. Michaelides, "Fast and accurate quantum Monte Carlo for molecular crystals," *Proc. Natl. Acad. Sci.*, vol. 0, p. 201715434, 2018.

O. Witham, R. J. Hunt, and N. D. Drummond, "Stability of trions in coupled quantum wells modeled by two-dimensional bilayers," *Phys. Rev. B*, vol. 97, no. 7, pp. 1–6, 2018.

S. B. Doma and A. A. Amer, "Ground-state calculations of confined hydrogen molecule  $\text{H}_2$  using variational Monte Carlo method Ground-state calculations of confined hydrogen molecule  $\text{H}_2$  using variational," vol. 8976, 2018.

N. Y. Astrakhantsev, V. V. Braguta, M. I. Katsnelson, A. A. Nikolaev, and M. V. Ulybyshev, "Quantum Monte Carlo study of electrostatic potential in graphene," *Phys. Rev. B*, vol. 97, no. 3, pp. 1–6, 2018.

J. Trail, B. Monserrat, and L. Pablo, "Quantum Monte Carlo study of the energetics of the rutile ,anatase ,brookite , and columbite  $\text{TiO}_2$  polymorphs," vol. 121108, 2017.

L. Q. Monte-carlo, "A benchmark study of  $\text{Li}_2^+$  ,  $\text{Li}_2^-$  ,  $\text{LiH}^+$  and  $\text{LiH}^-$ : Quantum Monte-Carlo and Coupled-Cluster computations," *Comput. Theor. Chem.*, 2017.

M. Szyniszewski, E. Mostaani, N. D. Drummond, and V. I. Fal, "Binding energies of trions and biexcitons in two-dimensional semiconductors from diffusion quantum Monte Carlo calculations," vol. 081301, pp. 1–5, 2017.

S. Nasiri and M. Zahedi, "Coupled Cluster and Quantum Monte-Carlo potential energy curves of the ground state of  $\text{Be}_2$  and  $\text{Be}_2^+$  molecules Saeed Nasiri and Mansour Zahedi \*," *Comput. Theor. Chem.*, 2017.

- M. Caffarel et al., "Communication : Toward an improved control of the fixed-node error in quantum Monte Carlo : The case of the water molecule Communication : Toward an improved control of the fixed-node error in quantum Monte Carlo : The case of the water molecule," vol. 151103, no. 2016, 2017.
- S. B. Doma and A. A. Amer, "Ground states of the hydrogen molecule and its molecular ion in the presence of a magnetic field using the variational Monte Carlo method," vol. 8976, no. March, 2016.
- W. Purwanto, S. Zhang, and H. Krakauer, "Auxiliary-field quantum Monte Carlo calculations of the molybdenum dimer," J. Chem. Phys., vol. 144, no. 24, 2016.
- A. D. Powell and R. Dawes, "Calculating potential energy curves with fixed-node diffusion Monte Carlo: CO and N2," J. Chem. Phys., vol. 145, no. 22, 2016.
- R. Nazarov, L. Shulenburger, M. Morales, and R. Q. Hood, "Benchmarking the pseudopotential and fixed-node approximations in diffusion Monte Carlo calculations of molecules and solids," Phys. Rev. B, vol. 93, no. 9, pp. 1-15, 2016.

